Acta Medica
Okayama

*Original Article*

# Design of Hemispherical Radio Frequency (RF) Capacitive-type Electrode Free of Edge Effects for Treatment of Intracavitary Tumors

Masahiro Moriyama[a]*, Atsuya Kawaguchi[a], Masaki Yokokawa[a], Shin Ikeda[a], Hajime Kitagaki[b], and Nobue Uchida[a]

*Departments of [a]Radiation Oncology and [b]Radiology, Faculty of Medicine, Shimane University, Izumo, Shimane 693–8501, Japan*

A new hemispherical electrode to heat oral cavity cancer is proposed. The electrode does not produce a hot spot around its edge, a feature that usually arises when using radio frequency (RF) capacitive-type heating. The hemispherical electrode was designed by computer simulation using a 3–D finite element method. To assess its practicality and effectiveness, we built a prototype hemispherical electrode and evaluated its heating characteristics by phantom experiments. The heating effects on the phantom were measured by thermography. The concave phantom surface in contact with the hemispherical electrode showed a uniform increase in temperature, with no obvious edge effect. The proposed electrode allows non-invasive RF capacitive-type heating for intracavity tumors that was not previously considered possible, and should contribute to the multidisciplinary treatment of intracavity tumors.

Key words: radiofrequency heating, capacitive-type heating, electrode, edge effect, hemispherical electrode

Radiotherapy or chemoradiotherapy is often preferable to surgery for head and neck cancers, for cosmetic reasons as well as functional preservation; however, while clinical outcomes of radiotherapy or chemoradiotherapy for head and neck cancer are improving, the results remain less satisfactory than those of surgical procedures [1]. The use of new cytotoxic agents, molecular targeting agents, and hyperthermia application techniques will be necessary to improve the clinical outcomes of head and neck cancer patients treated with chemoradiotherapy. A randomized phase III study of radiotherapy combined with intracavity hyperthermia versus radiotherapy alone for nasopharyngeal cancer revealed significantly better survival and tumor control with the former, while oral mucous toxicity in both arms was comparable [2].

In the case of oral cavity cancer, the addition of hyperthermia to radiotherapy or to chemoradiotherapy is also expected to achieve better clinical results. Invasive heating techniques are applied to heat the oral cavity, such as the implantation of ferromagnetic material, microwave interstitial heating, and the use of a bipolar radiofrequency electrode for interstitial ablation [3–5]. The distributions of the Specific Absorption Rate (SAR) and temperature produced by the inserted applicator are dependent upon the intra-applicator space and the depth of insertion, which are affected by the skill of the operator [6, 7]. A recent report about the clinical application of external heating to head and neck cancers includes a case of oropharyngeal cancer [8], but oral cavity cancers in

general cannot be heated effectively by external heating methods because the tumor is surrounded by air and a thick bony wall.

Radio frequency (RF) capacitive-type heating generates Joule heating by applying RF between two external electrodes, thereby raising the temperature of the human tissue through which the electric current passes. However, the electric current tends to concentrate in the tissue around the peripheral area of the electrode, inducing an edge effect and excessive heating [9–11]. The edge effect induces pain and fat necrosis, resulting in inadequate clinical results.

To prevent the induction of the edge effect, researchers and clinicians have applied many types of electrical-field (E-field)-modifying material between the electrode and the tissue to be heated, e.g., various forms of insulation on the electrode, or a water bag or bolus filled with saline solution [12]. However while these devices are generally acceptable from a clinical standpoint for heating the human trunk, the use of E-field-modifying material for heating a tumor localized in a limited space such as the oral cavity presents significant problems.

We previously designed an intracavitary RF capacitive-type heating electrode [13] that can heat tumor lesions directly and noninvasively, but hot spots arose near the edge of the electrode. We focused on creating an electrode shape that would allow a more uniform distribution of the electrical field, minimize the edge effect, and improve the treatment of oral cavity cancer. We devised a hemispherical-shaped electrode that does not produce an edge effect and that requires no E-field-modifying material such as an insulator or bolus. The heating characteristics were

evaluated using both computer simulation and agar phantom experiments.

## Materials and Methods

*Computer simulation (calculation model).* A cube-shaped muscle of $20 \times 20 \times 20 \, cm^3$ was positioned as the phantom in air. An example of the model is shown in Fig. 1. A pair of flat plate electrodes 1 mm thick made of aluminum with aluminum lead wires were placed on the top and bottom of the phantom. The electrodes were $5 \times 5 \, cm^2$ and $10 \times 10 \, cm^2$, respectively. When an electric potential with a frequency of 13.56 MHz and an amplitude of 100 V was applied to the pair of electrodes, the electric field and the SAR distributions were calculated using the finite element method software COMSOL Multiphysics (COMSOL, Inc., Stockholm, Sweden). The physical characteristics of the muscle phantom were an electric conductivity of $\sigma = 0.628 \, S/m$, a relative dielectric constant of $\varepsilon_r = 138.4$, and a density of $\rho = 1,070 \, kg/m^3$. In the simulation shown in Fig. 1A and 1B, various E-field-modifying materials were simulated by changing the electrical properties, configuration thickness, and coverage to prevent the induction of the edge effect.

*Phantom experiment using the prototype electrode.* A prototype hemispherical electrode was prepared to confirm the heating characteristics of the proposed electrode obtained in the simulation results. A phantom was embedded by the hemispherical electrode and heated with an RF current, and then the temperature distribution on the cross-section of the phantom was measured with a thermogram. The hemi-
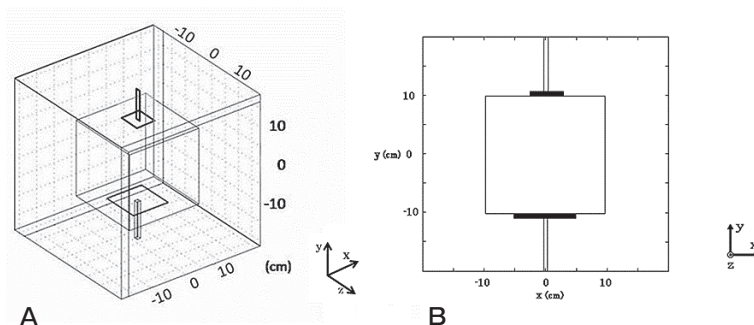


Fig. 1   Schematic diagram of simulation. A 5 × 5 cm flat plate small electrode on the top, and a 10 × 10 cm large electrode at the bottom of the cube-shaped muscle phantom, 20 × 20 × 20 cm. **A**, Orthographic projection; **B**, x-y view at z = 0.

spherical electrode and agar phantom are shown in Fig. 2. Fig. 2A shows the cross-section of the arrangement of the electrodes in the phantom. The hemispherical electrode was fabricated using aluminum foil for the electrode and was connected to a conductor wire. The surface of a 3–cm-radius rubber ball was covered with aluminum foil, and the upper half of the ball was then covered with insulating tape (Fig. 2B). An external electrode with a conductor wire was also prepared (Fig. 2B). The external electrode was made of aluminum and was $10 \times 10 \, cm^2$. A muscle-equivalent agar phantom of $15 \times 15 \times 13 \, cm^3$, composed of water (95.68 w/w %), NaCl (0.22 w/w %), $NaN_3$ (0.1 w/w %), and agar (4 w/w %), was prepared. The heating system was composed of a signal generator (8656B, Hewlett Packard Co.), an amplifier (L-1014, Tokyo Hy-Power Labs), and a matching box with power meter (AS-3001, Tokyo Hy-Power Labs). A thermographic recorder (INFI-2000, Nihon Kohden) was used to measure the temperature distribution on the surface of the phantom. The lower half of the hemispherical electrode was buried in the phantom (Fig. 2C). The phantom was then cut into 2 parts at the plane bisecting the concave area (Fig. 2D). The external electrode was placed under the phantom, and RF power was supplied for 2 min between the hemispherical electrode and the external electrode at a frequency of 9.0 MHz and an output power of 5 W. Ten sec after heating, the temperature distribution on the cutting surface of the phantom was recorded on a thermogram.

## Results

### *Results of computer simulation.*
### 1. Flat plate electrode

Fig. 3 shows the SAR distribution on the x-y plane at z = 0 cm. Fig. 3B is the magnified view of Fig. 3A. Fig. 3C shows the SAR profile along the x direction at y = 9.9 cm and z = 0 cm. The edge effect occurs near the edge of the electrode. The SAR contour takes the shape of a concentric circle with its center at the corner of the electrode.

Fig. 4 shows the SAR distribution when a polyethylene sheet ($\varepsilon_r = 2.3$, $\sigma = 0 \, S/m$) 1 mm thick (Fig. 4A) or 2 mm thick (Fig. 4B) is inserted between the flat plate electrode and the phantom. The edge effects arise in both of the simulations. When the thickness of the E-field-modifying material was increased to 2 mm, the edge effect was reduced slightly.

Fig. 5 shows the SAR distribution around the edge of the electrode on the x-y plane at z = 0 cm when the left edge of the flat plate electrode is covered with polyethylene ($\varepsilon_r = 2.3$, $\sigma = 0.0 \, S/m$), the cross-section
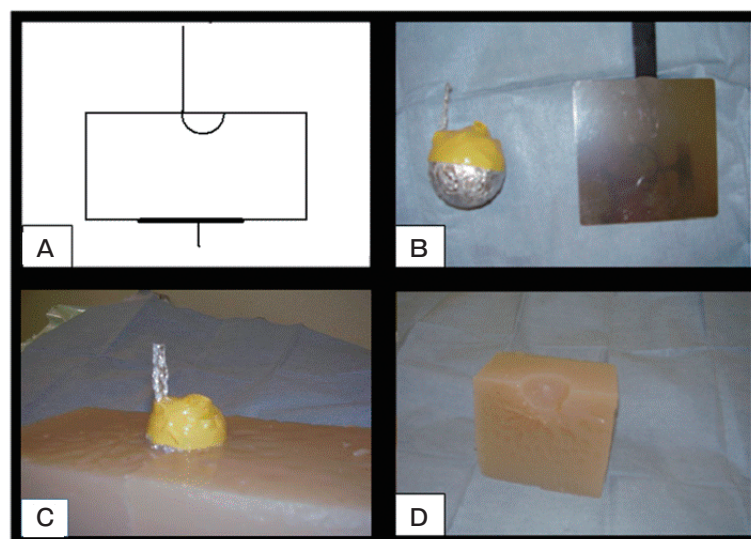


Fig. 2    Hemispherical electrode and agar phantom. **A**, Arrangement of electrodes and phantom; **B**, Hemispherical electrode (left) and external electrode (right); **C**, Hemispherical electrode buried in the top of the phantom; **D**, Bisecting plane of the phantom, which was measured with a thermographic recorder.
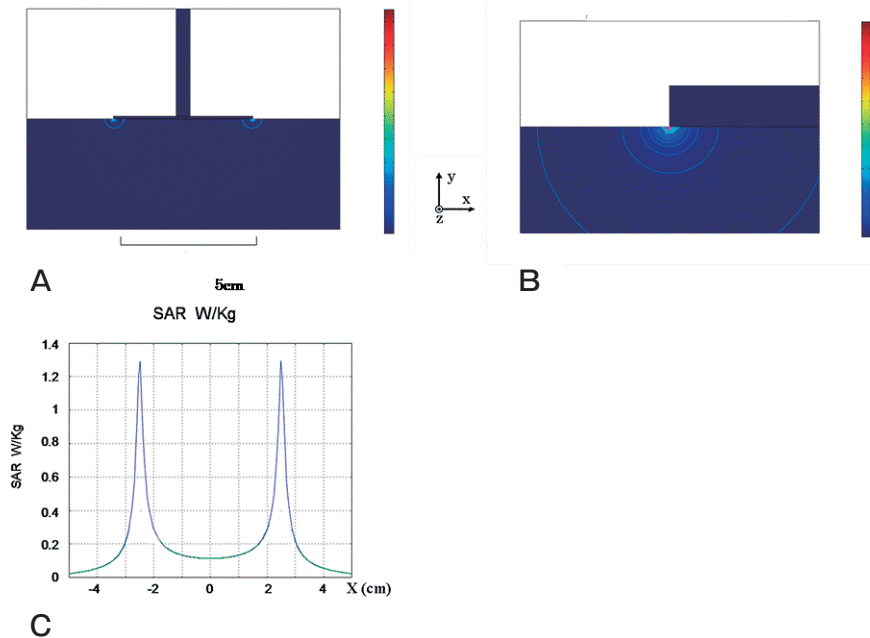
Fig. 3    SAR distribution when the flat plate electrode is placed on the phantom; **A**, SAR distribution on the x-y plane at z = 0 cm. Edge effects are seen around the end of the electrode; **B**, Magnified view of the end of the electrode; **C**, SAR profile along the x direction at the position of y = 9.9 cm, z = 0 cm.
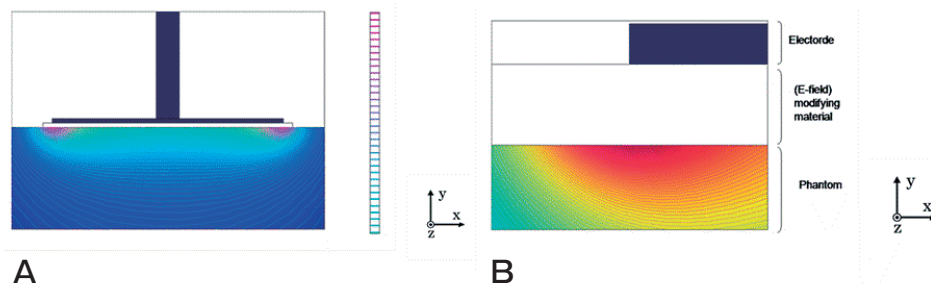


Fig. 4    SAR distribution when an E-field-modifying material is inserted between the flat plate electrode and the phantom; **A**, 1 mm thickness of E-field-modifying material (x-y plane at z = 0 mm); **B**, 2 mm thickness of E-field-modifying material (magnified view, x-y plane at z = 0 mm).

of which is elliptical. The edge effect arises around the junction of the electrode and the phantom. Because the use of any E-field-modifying material to solve the edge effect has limitations, we focused on reconfiguring the shape of the electrode.

## 2. Hemi-ellipsoidal electrode

Fig. 6 shows the SAR distribution when a hemi-ellipsoidal electrode is buried in the phantom. Fig. 6A shows the arrangement of the electrode, and Fig. 6B and 6C show the vector of the electric field around the hemi-ellipsoidal electrode on the x-y plane at

z = 0 cm.

Fig. 6D shows the SAR distribution on the x-y plane at z = 0 cm. No edge effect arises at the edge of the electrode, and a relatively higher SAR arises around the electrode. A strong SAR occurs around the convex part of the electrode.

## 3. Hemispherical electrode

Fig. 7 shows the SAR distribution on the x-y plane at z = 0 cm when a hemispherical electrode is buried in the phantom. Fig. 7A shows the arrangement of the electrodes, in which the radius of the
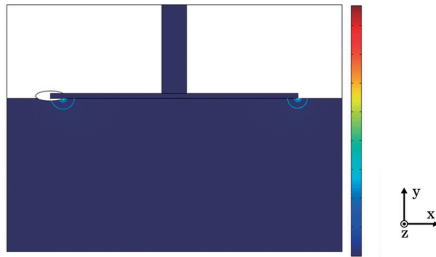
**Fig. 5**    SAR distribution when the left edge of the flat plate electrode is covered with a polyethylene E-field-modifying material. The cross-sectional shape of the material is elliptical.

electrode is 2.5 cm. Fig. 7B and 7C show the vector of the electric field around the hemispherical electrode on the x-y plane at z = 0 cm in a magnified view.

Fig. 7D shows the SAR distribution on the x-y plane at z = 0 cm. No edge effect arises around the edge of the hemispherical electrode, and the SAR distribution is uniform along the electrode surface. The SAR distribution decreases gradually with the distance from the surface of the electrode. Fig. 7E shows the SAR distribution on the z-x plane at y = 9.9 cm. The SAR distribution is uniform along the electrode surface, and the SAR decreases with the distance from the surface of the hemispherical electrode. The SAR ratio calculated from Fig. 7 was 94% at 5 mm depth, 88% at 10 mm depth, 77% at 15 mm depth, and 71% at 20 mm depth, when assuming the SAR of the surface of the electrode was 100%.

### *Results of the phantom experiment.*

Fig. 8 shows the temperature distribution on the surface of the bisecting plane. The thermogram shows a uniform temperature rise along the concave surface. The pattern of the temperature rise indicates the aspect of a concentric circle, and the temperature rise decreases with the depth from the concave surface.

## Discussion

***Occurrence of the edge effect.***    The simulations for an edge effect arising in capacitive-type heating revealed that 1) insertion of a sheet of E-field-modifying material at the border of the electrode and the phantom could not eliminate the edge effect, even after changing the thickness, shape, and dielectric property of the E-field-modifying material, 2) enfolding the electrode by E-field-modifying material could

not eliminate the edge effect, even after changing the thickness and shape of the E-field-modifying material, 3) the hemi-ellipsoidal electrode did not induce the edge effect, but the SAR distribution along the electrode was not uniform, 4) the hemispherical electrode did not induce the edge effect and the SAR distribution along the electrode was uniform.

In RF capacitive-type heating with a pair of flat plate electrodes, the edge effect arises at the peripheral areas of the electrodes [10–12]. The edge effect causes a hot spot in the heated area, focal pain, and fat necrosis, resulting in an insufficient temperature rise or inadequate clinical results [14, 15]. To prevent the induction of the hot spot, clinicians often use E-field-modifying material filled with saline solution, or a bolus, to create a distance between the electrode and the heated body. Another procedure is to circulate saline solution in a bolus to lower the surface temperature of the body [16]. An electric insulator as an E-field-modifying material is sometimes applied to the peripheral area of the electrode. When heating in a limited space such as an oral cavity, however, electrodes incorporating some form of insulator are too large for practical clinical use. The cold saline solution circulation bolus is also too large to be useful for tumors developing in a localized space such as the oral cavity.

***Measures against the edge effect: E-field-modifying material.***    We used simulation to examine the efficacy of various types and shapes of E-field-modifying materials to reduce the edge effect. When the thickness of the E-field-modifying material increases, the edge effect decreases, but the edge effect remains around the edge of the electrode, as shown in Fig. 4. When the edge of the electrode was covered with a non-conductive E-field-modifying material, the cross-sectional shape of which was elliptical, the edge effects arose around the junction of the electrode and the phantom, as shown in Fig. 5. Even though the dielectric properties of the E-field-modifying material were changed, the edge effect did not disappear. When the RF current flows across the boundary at which 2 materials having different dielectric properties to each other are contacted, it is refracted, which can produce a concentration of RF current. Thus, the changes of shape and dielectric property of the E-field-modifying material failed to eliminate the edge effect.
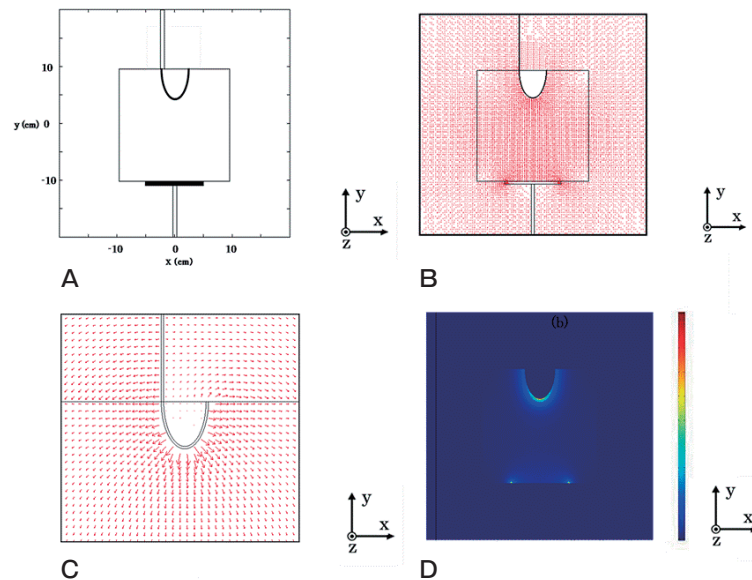
**Fig. 6**    SAR distribution when a hemi-ellipsoidal electrode is buried in the phantom; **A**, Arrangement of the hemi-ellipsoidal electrode; **B**, The vector of the electric field around the hemi-ellipsoidal electrode on the x-y plane at z = 0 cm; **C**, Magnified view on the x-y plane at z = 0 cm; **D**, SAR distribution on the x-y plane at z = 0 cm.

***Measures against the edge effect: electrode shapes.***    A point/cup electrode is generally used to prevent corona discharge in the area of high voltage transmissions, and the edge of the point/cup electrode is rounded. The electric flux density is concentrated around the point of the electrode, which has a small radius of curvature, and the intensity of the electric field is strengthened. The direction of the electric flux is vertical with respect to the surface of the electrode, and the strength of the electric field around the edge of the electrode would become smaller if the electrode had a larger radius of curvature.

As shown in Fig. 6B and 6C, the normal vector at the edge of the semi-ellipsoidal electrode is parallel to the surface of the phantom and the radius of curvature around its edge is large, so that the edge effect does not appear around the edge of the electrode, as shown in Fig. 6D. The radius of curvature around the bottom of the electrode is small compared with the area around the edge of the electrode, so that the SAR around the bottom of the electrode is high compared with that around the edge of the electrode.

To maintain uniform current density around the electrode, the curvature radius of the electrode must be uniform at all points on the electrode. Fig. 7 shows the SAR distribution using the hemispherical electrode. The normal vector at the edge of the hemispherical electrode is parallel to the surface of the phantom and the radius of curvature at any point of the hemispherical electrode is identical (Fig. 7B and 7C), so that the SAR along the hemispherical electrode is identical. The phantom experiments shown in Fig. 8 confirmed that the edge effect was not induced when the hemispherical electrode was used for RF capacitive-type heating.

***Clinical indications of the hemispherical electrode.***    In hyperthermia for oral cavity cancer, various kinds of heating methods and devices such as implantation of ferromagnetic material [3], microwave interstitial heating [4], and bipolar radiofrequency electrode for interstitial ablation [5] have been applied. A recent report about the clinical application of external heating to head and neck cancers includes a case of oropharyngeal cancer [8], but in general oral cavity cancer cannot be heated effectively by external heating methods, because the tumor is surrounded by air and a thick complicating bony wall. A non-invasive, effective direct heating device for oral cancer is required. To our knowledge, there have been no prior reports of a hemispherical electrode that does not generate an edge effect.

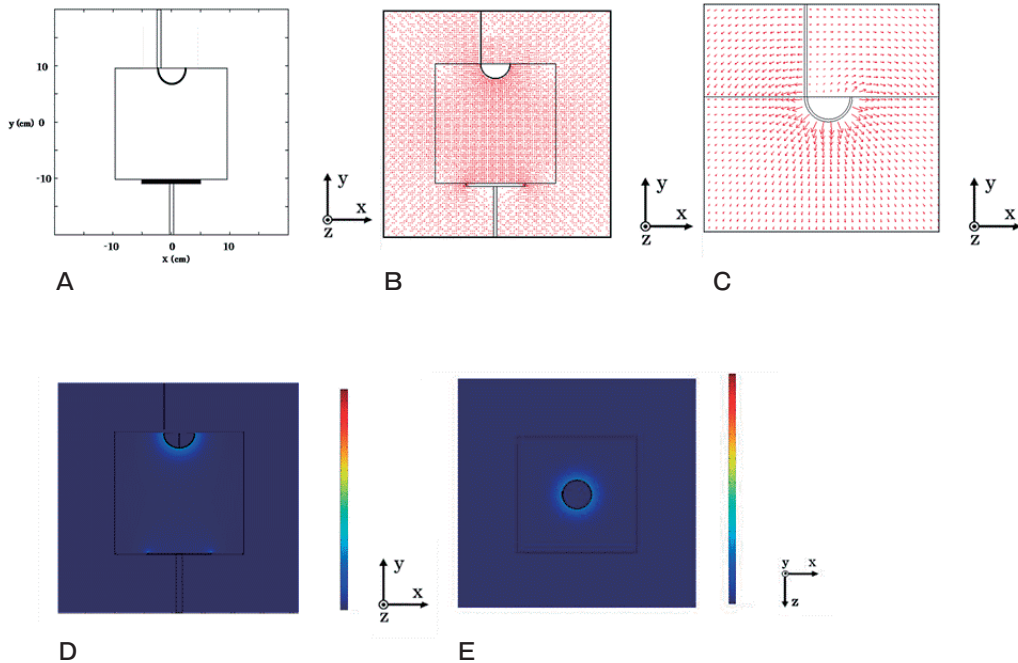The RF capacitive-type heating advantage of deep

Fig. 7    SAR distribution when a hemispherical electrode is buried in the phantom;  **A**,  Arrangement of the hemispherical electrode;  **B**, The vector of the electric field around the hemispherical electrode on the x-y plane at z = 0 cm;  **C**,  Magnified view on the x-y plane at z = 0 cm;  **D**,  SAR distribution on the x-y plane at z = 0 cm;  **E**,  SAR distribution on the z-x plane at y = 9.9 cm.
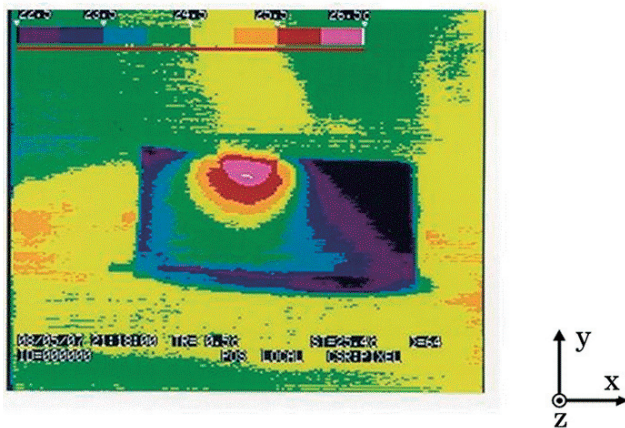


Fig. 8    Thermogram of the surface of the bisecting plane.

penetration is limited by the edge effect,  thus reducing its clinical usefulness. In this study,  we developed a hemispherical electrode that does not cause the edge effect. We have confirmed the heating characteristics of RF capacitive-type heating with the new hemispherical electrode through computer simulation and phantom experiments. The proposed hemispherical electrode can be used for noninvasive heating,  and its distinguishing shape permits placement adjacent to intracavity tumors within cavities such as the mouth and vagina.

While the SAR ratio distribution is not sufficient to heat a deep-seated tumor or large tumor with a thickness greater than 10 mm,  a possible solution to overcome this problem,  though untested,  could be a cyclical cooling saline bolus situated on the concave surface of the hemispherical electrode. This remedy would likely make it feasible to raise the input power. Furthermore,  while insufficient contact between an electrode and a mucosal surface produces hot spots,  a saline gel applied for better contact serves to minimize such overheating. This would also permit the increase of input power.

Prior to the application of this electrode for head and neck cancer treatment,  further research is necessary. However,  the results of the present study indicate that a hemispherical electrode that solves the edge effect problem,  which is the weak point of RF capacitive-type heating,  could expand the indication for RF capacitive-type heating. An example of this might be concomitant thermoradiotherapy with a remote afterloading system (RALS),  as has been previously

proposed [13]. This mold type electrode can provide RF hyperthermia and brachytherapy concomitantly.

In conclusion, a hemispherical electrode that generates no edge effect was developed to allow noninvasive heating of intracavity tumors for which RF capacitive-type heating was generally considered unavailable. This method is expected to make a significant contribution to the multidisciplinary treatment of intracavity tumors.

## References

1. Soo KC and Tan EH: Surgery and adjuvant radiotherapy vs concurrent chemoradiotherapy in stage III/IV nonmetastatic squamous cell head and neck cancer: a randomized comparison. Br J Cancer (2005) 93: 279–286.
2. Hua Y, Ma SL, Fu ZF, Hu QY, Wang L and Piao YF: Intracavity hyperthermia in nasopharyngeal cancer: A phase III clinical study. Int J Hyperthermia (2011) 27: 180–186.
3. Tohnai I, Goto Y, Hayashi Y, Ueda M, Kobayashi T and Matsui M: Preoperative thermochemotherapy of oral cancer using magnetic induction hyperthermia (Implant Heating System: IHS). Int J Hyperthermia (1996) 12: 37–47.
4. Prevost B, De Cordoue-Rohart S, Mirabel X, Camart JC, Fabre JJ, Szanski JP and Chive M: 915 MHz microwave interstitial hyperthermia. Part III: Phase II clinical results. Int J Hyperthermia (1993) 9: 455–462.
5. Liukko T, Makitie AA, Markkola A, Ylikoski J and Back L: Radiofrequency induced thermotherapy: an alternative pal treatment modality in head and neck cancer. Eur Arch Otorhinolaryngol (2006) 263: 532–536.
6. Denman DL, Elson HR, Lewis GC, Breneman JC, Clausen CL, Dine J and Aron BS: The distribution of power and heat produced by interstitial microwave antenna arrays: I. Comparative phantom and canine studies. Int J Radiat Oncol Biol Phys (1988) 14: 127–137.
7. Sundararaman S, Denman DL, Legorreta RA, Foster AE, Redmond KP, Elson HR, Bom AM, Samaratunga RC, Lewis GC Jr and Kereiakes JG: The modification of specific absorption rates in interstitial microwave hyperthermia via tissue-equivalent material bolus, Int J Radiat Biol Phys (1990) 19: 677–685.
8. Paulides MM, Bakker JF, Linthorst M, Van der Zee J, Rijinen Z, Neufeld E, Pattynama PMT, Jansen PP Levendag PC and Van Rhoon GC: The clinical feasibility of deep hyperthermia treatment in the head and neck: new challenges for positioning and temperature measurement. Phys Med Biol (2010) 55: 2465–2480.
9. Jeffrey WH and James RJ: Physical techniques in clinical hyperthermia. 1 st Ed, Research Studies Press, Letchworth (1986) pp 98–137.
10. Van der Zee J, Vujaskavic Z, Kondo M and Sugahara T: The Kadota Fund International Forum 2004-Clinical group consensus. Int J Hyperthermia (2008) 24: 111–122.
11. Kato H, Uchida N, Kasai T and Ishida T: A new applicator utilizing distributed electrodes for hyperthermia: a theoretical approach. Int J Hyperthermia (1995) 11: 287–294.
12. Kroeze H, Van Vulpen, De Leeuw AAC, Van de Kamer JB and Lagendijk Jan JW: Improvement of absorbing structures used in regional hyperthermia. Int J Hyperthermia (2003) 19: 598–616.
13. Moriyama M, Uchida N, Kitagaki H, Kato H, Mishima K and Yoshimura Y: Development of a new mould-type RF-hyperthermia electrode for oral cancer. 8th International Congress of Hyperthermic Oncology, proceedings, Kyongju (2000).
14. Kato H, Furukawa M, Uchida N, Kasai T and Ishida T: A new capacitive-type heating method inducing less heat in fat layers. Jpn J Hyperthermic Oncol (1991) 7: 452–454.
15. Kato H, Kuroda M, Shibuya K and Kanazawa S: Focused deep heating with an inductive type applicator. Thermal Med (2007) 23: 133–143.
16. Overgaard J: The current and potential role for hyperthermia in radiotherapy. Int J Radiat Oncol Biol Phys (1989) 16: 535–549.